ARTICLE

Wide Contact Structures for Low-Noise Nanochannel Devices Based on a Carbon Nanotube Network

Hyungwoo Lee,[†] Minbaek Lee,[†] Seon Namgung,[†] and Seunghun Hong[†,‡,*]

[†]Department of Physics and Astronomy, Seoul National University, Seoul 151-747, Korea, and [‡]Department of Biophysics and Chemical Biology (WCU Program), Seoul National University, Seoul 151-747, Korea

ABSTRACT We have developed a wide contact structure for low-noise nanochannel devices based on a carbon nanotube (CNT) network. This low-noise CNT network-based device has a dumbbell-shaped channel, which has wide CNT/electrode contact regions and, in effect, reduces the contact noise. We also performed a systematic analysis of structured CNT networks and established an empirical formula that can explain the noise behavior of arbitrary-shaped CNT network-based devices including the effect of contact regions and CNT alignment. Interestingly, our analysis revealed that the noise amplitude of *aligned* CNT networks behaves quite differently compared with that of *randomly oriented* CNT networks. Our results should be an important guideline in designing low-noise nanoscale devices based on a CNT network for various applications such as a highly sensitive low-noise sensor.

KEYWORDS: carbon nanotube · 1/*f* noise · low frequency noise · contact resistance · aligned network

Carbon nanotubes (CNTs) have been considered as a promising material for high-performance functional devices such as high-speed field-effect transistors (FETs)[1−5] and highly sensitive sensors.[6−8] A key parameter determining device performance can be its noise level.[9] Previous works show that CNT-based devices have a rather large 1/*f* noise compared to conventional semiconducting devices, and the noise amplitude A for the devices based on a bulk CNT network channel was proportional to the resistance R of the CNT-based device like $A \sim 10^{-11} \times R$.[10,11] In the case of rectangular-shaped CNT network channels, the channel width and length were reported to affect the noise behavior.[12,13] However, most of previous studies were about CNT network channels much larger than the length of individual CNTs. On the other hand, recent reports showed that CNT networks can be aligned using the nanoscale-wide molecular patterns. Furthermore, the FETs and sensors based on the aligned CNT networks in the nanoscale-wide channels exhibited improved mobility and sensitivity compared with those based on random CNT networks, respectively.[14,15] However, increased noise of nanochannel devices can be a major hurdle for its practical applications, and we do not even have a model to describe the noise characteristics of nanoscale channel width devices.

Herein, we developed a wide contact structure for low-noise nanochannel devices based on CNT networks and also report an empirical formula to describe the noise characteristics of structured CNT network channels. This CNT network-based device has a dumbbell-shaped CNT network channel composed of a narrow long channel region and wide CNT/electrode contacts. The wide contact device exhibited relatively small noise compared to a conventional device with rectangular-shaped channels. In addition, we established an empirical formula that can describe the noise behavior of CNT network-based devices, including the effect of contact regions and aligned CNT networks. Interestingly, the systematic noise analysis on our devices shows that the noise characteristics of *aligned* CNT networks are quite different from that of *randomly oriented* CNT networks. This result can provide a key strategy to design low-noise high-performance devices based on CNT networks.

RESULTS AND DISCUSSION

The CNT network-based FET arrays were fabricated following the directed assembly strategy as reported before (Supporting Information Figure S1).[16−18] In brief, a photoresist (PR) was patterned on the SiO_2 substrate, and the PR-patterned substrate was dipped into octadecyltrichlorosilane (OTS)

*Address correspondence to seunghun@snu.ac.kr.

Received for review September 6, 2010 and accepted October 29, 2010.

Published online November 4, 2010. 10.1021/nn102296e

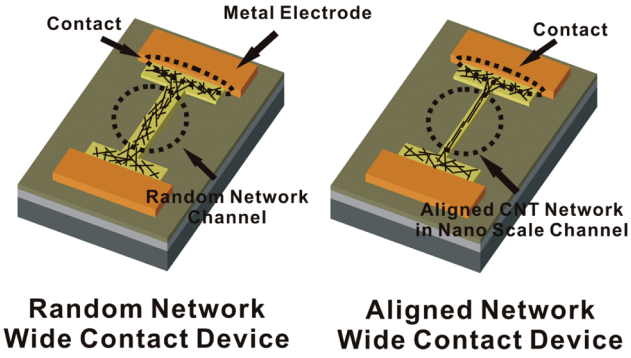

Figure 1. Schematic diagram depicting the structure of wide CNT/electrode contact device. The geometry (width) of CNT/electrode contact plays a crucial role in our noise model to reduce noise amplitude. This wide contact structure was also applied to the nanoscale channel (right).

solution (1:500 v/v concentrations in anhydrous hexane) to form nonpolar molecular patterns on the bare SiO_2 regions without PR. Then, the substrate was dipped into the SWNT (HiPCo, Carbon Nanotechnologies Inc.) suspensions (0.01 mg/mL in *o*-dichlorobenzene), subsequently rinsed with *o*-dichlorobenzene, and dried by nitrogen gas. In the SWNT suspensions, SWNTs were adsorbed onto the bare SiO_2 regions and aligned to stay inside the regions. Note that, in case of nanoscale-wide SiO_2 regions, the adsorbed SWNTs were rotated to stay in the SiO_2 regions, and as a result, they were highly aligned along the channel direction.[16] Last, the metal electrode (Ti/Au) was fabricated by photolithography, thermal evaporation, and lift-off process. We prepared two types of *wide contact* CNT network-based FETs (Figure 1): wide contact devices with a randomly oriented CNT network-based microscale-wide channel or an aligned CNT network-based nanoscale-wide channel. The noise spectra of the fabricated CNT network devices were measured using a Stanford Research Systems model SR 570 current preamplifier and SR 770 FFT network analyzer.

Figure 2a shows the AFM topography image of a channel based on a randomly oriented CNT network. The channel width is 2 μm, and the contact width ranges from 2 to 100 μm. As expected, the resistance of device decreased as the contact width increased (Figure 2b). In our fabrication process, we could reproducibly achieve a uniform monolayer of CNT networks due to the "self-limiting" mechanism where first-adsorbed CNTs blocked the additional adsorption.[16,17] In this case, CNT adsorption followed the Langmuir isotherm-like behavior, and the uniformity of the adsorbed CNT monolayer was highly reproducible.[14,30] Therefore, we can assume the CNT random network as a uniform film, and the resistance of the device can be written by

$$R_{total} = R_{ch} + 2R_{cont} = \rho_{ch}\sum\frac{L}{a} + \frac{r_{cont}}{W} \qquad (1)$$

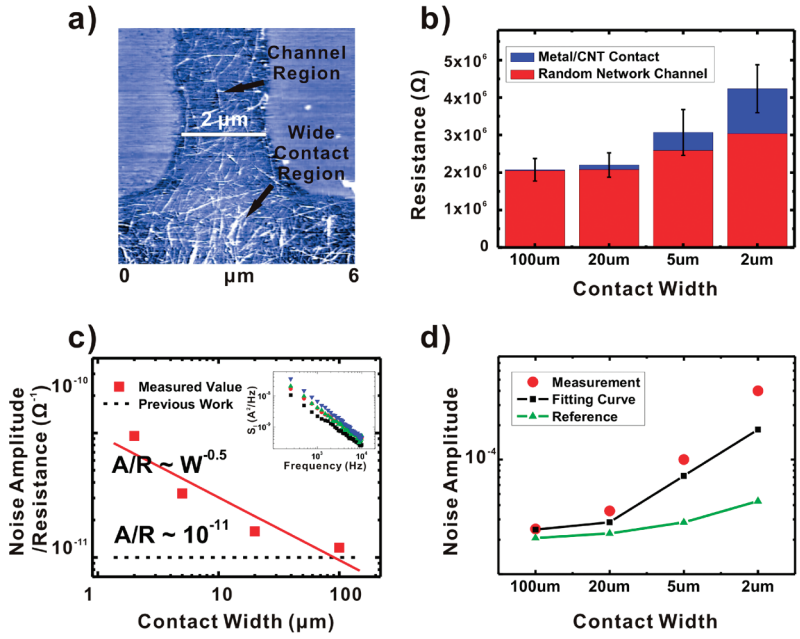

Figure 2. (a) AFM topography of a wide contact device with a 2 μm wide random network channel. The lower part of image shows the wide contact region. (b) Estimated contact and channel resistance values of random network devices with various contact width *W*. An averaged measurement result of eight or more samples with the corresponding standard error is shown. (c) Ratio of noise amplitude (*A*)/resistance (*R*) for devices with various contact width *W*. The dashed line represents $A/R = 10^{-11}$ graph for CNT devices as reported before. Note that *A*/*R* is proportional to $W^{-0.5}$. The inset shows a typical behavior of 1/*f* noise. (d) Measured noise amplitude values (red circle) and theoretical fitting (black line) of random network devices. Green line represents the values estimated using the previous equation of $A = 10^{-11} \times R$ as reported previously. A power spectral density of a random network device was measured at 0.1 V as a drain−source bias.

where R_{ch}, R_{cont}, ρ_{ch}, L, a, r_{cont}, and W represent the channel resistance, contact resistance between metal electrodes and CNT networks, the resistivity of CNT random network, the channel length, the cross-sectional area of the channel, the prefactor of the width-dependent term, and the contact width, respectively. We assumed that the contact resistance is inversely proportional to contact width W with r_{cont} as a prefactor. We fabricated devices with different contact widths (contact width of 100, 20, 5, and 2 μm) and fitted the measured resistance values using eq 1 to estimate the r_{cont} and ρ_{ch} (Supporting Information). The r_{cont} and ρ_{ch} were estimated as 2.58 $\times 10^6$ and 269 $\Omega \cdot \mu$m, respectively. It allowed us to estimate the channel and contact resistances of our devices (Figure 2b).

Our CNT devices exhibited typical 1/*f* noise spectrum (inset of Figure 2c).[19] The measured noise power spectral density ($S_I = \langle \Delta I^2 \rangle$) followed the equation of $S_I = A(I^2/f^\delta)$, where the exponent δ is estimated to be ~1. Figure 2c shows the noise amplitude to resistance ratio (A/R) with various contact width W. Previous reports show that $A/R \sim$ constant ($\sim 10^{-11}$).[10] However, we found $A/R \sim W^{-0.5}$ for our devices with a structured channel. Specifically, in case of 100 μm width contact, the contact resistance is negligible compared with the channel resistance, and A/R ratio is actually close to 10^{-11} as reported previously (Figure 2b,c).[10] In the case of narrow contact devices, the contact resistance became a significant portion of the total device resistance, and the A/R ratio increased significantly from the constant value. This result shows that, when the contact resistance is rather large, a significant portion of noise may be originated from the contact between the electrodes and CNT networks.

Figure 2d shows the measured noise amplitude values (red dots) of the devices with various contact widths. Each point represents the averaged value of ~10 devices. The green dots represent the values calculated by the previously reported equation $A = 10^{-11} \times R$ and the measured resistance. Note that they matches well only for the 100 μm contact width devices when the contact resistance is relatively small compared with total resistance, while they deviate significantly for rather narrow contact width devices. It indicates that the contact between CNTs and electrodes generates a significant noise, which should be considered for narrow channel devices. We utilized an empirical model to estimate the characteristics of noise originated from contact resistance. Since the contact and channel resistances are connected in series as, the total noise amplitude A_{total} can be written as

$$A_{total} = A_{R_{ch}}\left(\frac{R_{ch}}{R_{total}}\right)^2 + 2A_{R_{cont}}\left(\frac{R_{cont}}{R_{total}}\right)^2 \quad (2)$$

where $A_{R_{ch}}$ and $A_{R_{cont}}$ represent the noise amplitude of CNT network channels and contact parts, respectively.[20] Since previous works show that $A_{R_{ch}}/R_{ch} \sim$ constant, we assumed that $A_{R_{ch}} = \alpha \times R_{ch}$, where α is a constant. However, since the characteristics of the noise amplitude $A_{R_{cont}}$ are still unknown, we assumed that $A_{R_{cont}} = \beta \times R_{cont}^{\gamma}$, where β and γ are unknown constants. Then, we can rewrite eq 2 as

$$A_{total} = \alpha R_{ch}\left(\frac{R_{ch}}{R_{total}}\right)^2 + 2\beta R_{cont}^{\gamma}\left(\frac{R_{cont}}{R_{total}}\right)^2 \quad (3)$$

We measured the total noise amplitude values of ~40 devices with different contact widths and fitted the data using eq 3 to estimate the values of α, β, and γ. The fitting results show that

$$A_{R_{ch}} \sim 1.21 \times 10^{-11} R_{ch} \quad (4)$$

$$A_{R_{cont}} \sim 7.39 \times 10^{-3} R_{cont}^{0.008} \quad (5)$$

Note that eq 4 is similar to the previous result, $A/R \sim 10^{-11}$, of rather large-scale CNT network channels. On the other hand, eq 5 shows that the characteristics of noise originated from the electrode−CNT contact, which has been ignored in previous works. Note that the noise amplitude $A_{R_{cont}}$ of the contact resistance is not affected much by the contact resistance. Previous work shows that the noise amplitude $A_{R_{cont}}$ ($= f \cdot (S_{R_{cont}}/R_{cont}^2)$) of perfect Ohmic contact does not depend on the contact resistance.[21] Presumably, the nonzero exponent 0.008 in our case can be attributed to nonperfect Ohmic contact of our devices.[22,23] The contact noise was usually ignored in previous works using rather larger scale channel devices. However, it can have a significant effect for the narrow and short channel devices which have a relatively large portion of contact resistance. The black line represents the fitting results based on our eqs 3, 4, and 5, indicating a good fit for the measured data. This result clearly shows that the contact resistance which generates additional random fluctuation should be considered to properly estimate the noise characteristics of small-scale devices.

We also investigated the effect of gate bias voltage V_g on the noise from channels and contacts (Figure 3). First, the noise amplitudes of random network devices with 2 and 100 μm contact width were measured under different gate bias voltages (Figure 3a). The back-gate bias voltage was applied using the underlying p-doped Si substrates. As reported previously, due to the semiconducting CNTs in the CNT network channels, the channel resistance R is a function of gate bias V_g as in $R = R(V_g)$.[1−3] Our results show that the positive gate bias V_g resulted in reduced source−drain current I_{ds} and, thus, increased channel resistance $R(V_g)$. It is a typical p-type gating behavior of CNT network junctions under ambient conditions as reported previously (Figure 3a).[3] Also note that the noise amplitude A increased

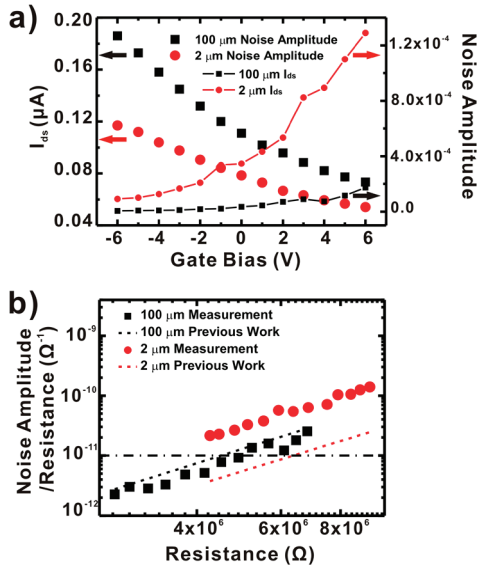

Figure 3. (a) Device current I_{ds} and noise amplitude A as a function of gate voltage for the wide contact (contact width ~100 μm) and normal contact (contact width ~2 μm) device. Both samples show a typical response of p-type FET. However, the 100 μm wide contact device shows smaller noise amplitude than the normal contact (2 μm wide) device. During the gate voltage sweeping, 0.5 V drain to source bias was applied to the device. (b) A/R of wide contact (black square) and normal contact device (red circle) *versus* resistance. Note that this behavior is a typical characteristic of the 1/*f* noise in percolating systems.[24,28] Dashed line represents the reference data reported before.

as the resistance increased by the positive gate bias voltages. Figure 3b shows the noise amplitude values at different source−drain resistances $R(V_g)$. The devices with 100 and 2 μm contact widths can be fitted by $A \sim 10^{-26.8} \times [R(V_g)]^{3.51}$ and $A \sim 10^{-27.8} \times [R(V_g)]^{3.44}$, respectively. Note that both devices exhibited a similar exponent to previously reported values.[19] In the case of 2 μm width devices, a significant portion of the noise came from the metal−CNT contacts, while the noise of 100 μm width devices came mainly from CNT channels. The similar exponent values for both 2 and 100 μm contact widths indicate that the noises from channels and contacts had a similar gate bias dependence. It indicates that the mechanism of noise from the CNT network channels is the same as that from contact. Presumably, the noise source of CNT networks is the contact between individual CNTs, thus exhibiting similar characteristics as the noise from metal−CNT contact.[12]

We performed a similar noise analysis for aligned CNT network channels (Figure 4a). In this case, the channel width is 100 nm, and the contact width ranges from 100 nm to 10 μm. Note that CNTs in the nanochannel region are aligned along the channel direction, while those in the wide contact region are randomly oriented as mentioned above (Supporting Information Figure S2). More quantitative analysis of CNT alignment in narrow and wide channels can be found in our previous works.[14,15] In brief, the degree of CNT alignment in CNT network channels can be measured quantitatively *via* Raman spectroscopy using the polarized laser light. We observed the larger Raman signals for CNT network channels when more CNTs were aligned along the polarization direction of the laser

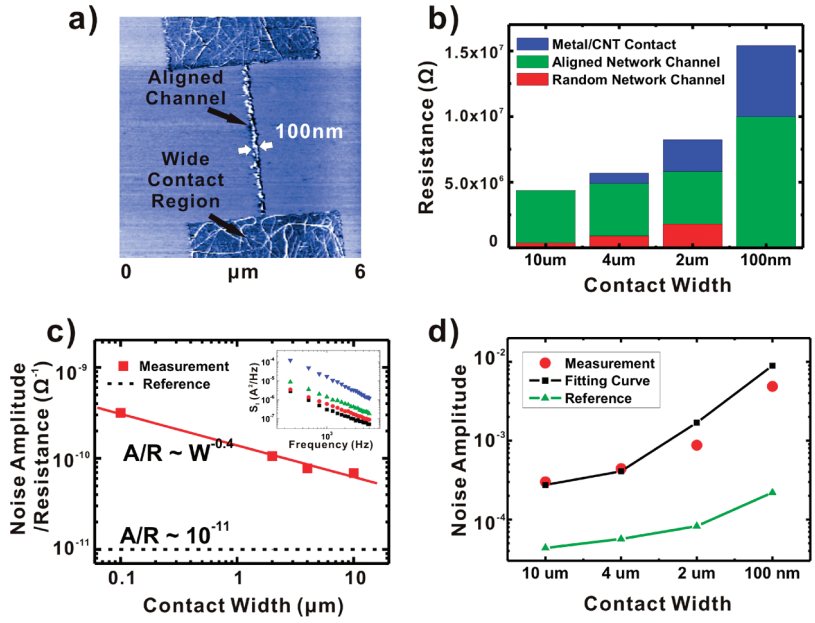

Figure 4. (a) AFM topography of a wide contact aligned network device. Note that the width of channel is 100 nm, and CNTs in this nanochannel were aligned along the channel direction. (b) Estimated contact and channel resistance values of the aligned network devices with various contact width W. The resistance of device comprises metal/CNT contact (blue), random network channel (red), and aligned network channel (green). (c) A/R as a function of contact width W. The inset shows a typical behavior of 1/*f* noise. Note that A/R is proportional to $W^{-0.4}$, and this noise behavior is almost the same with random network devices. (d) Measured noise amplitude values (red circle) and theoretical fitting (black line) of the aligned network devices. Green line represents the values estimated using the previously reported equation of $A = 10^{-11} \times R$. A power spectral density of a random network device was measured at 1.0 V drain to source bias with −6.0 V gate bias.

light. Furthermore, as CNTs were aligned along the channel direction, the conductivity and mobility of the channels were observed to increase continuously without any sharp transition.[14,15]

In the case of aligned CNT network devices, the devices were turned off at zero gate bias voltage due to the increased probability of semiconducting paths as reported previously.[14] Since we cannot get electric currents large enough for noise analysis at zero gate bias, we turned on the device with −6 V gate bias and performed the electrical characterizations of resistance and noise (Figure 4b−d). The resistance R_{total} of the device at −6 V gate bias can be written as

$$R_{total} = R_{a\_ch} + 2R_{r\_ch} + 2R_{cont} = \rho_{a\_ch}\left(\frac{L}{a}\right)_{a\_ch} + 2\rho_{r\_ch}\left(\frac{L}{a}\right)_{r\_ch} + \frac{r_{cont}}{W} \quad (6)$$

where the subscripts a_ch and r_ch represent the aligned and randomly oriented CNT network channel regions, respectively. R, ρ, L, and a represent the resistance, resistivity, length, and cross-sectional area of the corresponding channel regions marked by subscripts, respectively.

We fabricated devices with different contact widths (10, 4, 2 μm and 100 nm) and fitted the measured resistance values using eq 6 to estimate the ρ_{a_ch} and ρ_{r_ch} (Supporting Information). Here, r_{cont} was estimated as $1.37 \times 10^6\ \Omega \cdot \mu m$ from the microscale random network channels with −6 V gate bias, and it was used as a constant during the fitting process. The fitting results show that ρ_{r_ch} and ρ_{a_ch} are 604.4 and 99.9 $\Omega \cdot \mu m$, respectively. From these values, we can estimate the resistance of channels and contacts (Figure 4b).

Figure 4c shows A/R with various contact width. We found $A/R \sim W^{-0.4}$, where the scaling factor −0.4 was almost the same as that for random CNT network devices (Figure 2c). In the case of the devices with 10 μm wide contact, the resistance of the contacts and random CNT network regions is negligible, and most of the noise came from aligned CNT networks. Note that the A/R value for those devices with 10 μm wide contact is much larger than that of random CNT networks ($\sim 10^{-11}$), indicating that the noise from aligned CNT networks is larger than randomly oriented CNT networks with the same resistance values (Figure 4c).

Figure 4d shows the measured noise amplitude values (red dots) of the devices with various contact widths. The green dots represent the values estimated from the previously reported equation $A = 10^{-11} \times R$ and the measured resistance values. Note that the noise amplitude of aligned network devices deviated significantly from that of random network devices for all contact widths. It indicates that the aligned CNT network-based channels have noise characteristics quite different from random CNT network-based channels.

We utilized the similar empirical model (eqs 2 and 3) to estimate the noise characteristics of aligned CNT network channels. Here, the channel part was composed of random and aligned CNT networks. Then total noise amplitude can be rewritten as

$$A_{total} = A_{R_{\alpha\_ch}}\left(\frac{R_{a\_ch}}{R_{total}}\right)^2 + 2A_{R_{r\_ch}}\left(\frac{R_{r\_ch}}{R_{total}}\right)^2 + 2A_{R_{cont}}\left(\frac{R_{cont}}{R_{total}}\right)^2 \quad (7)$$

where $A_{R_{a\_ch}}$ and $A_{R_{r\_ch}}$ represent the noise amplitude of aligned and randomly oriented CNT network channels, respectively. We fitted the data in Figures 3b and 4d following the procedure in Supporting Information and found that

$$A_{R_{r\_ch}} \sim 1.14 \times 10^{-12} R_{r\_ch} \quad (8)$$

$$A_{R_{cont}} \sim 6.88 \times 10^{-4} R_{cont}^{0.28} \quad (9)$$

$$A_{R_{a\_ch}} \sim 1.77 \times 10^{-31} R_{a\_ch}^{4.14} \quad (10)$$

These results have several interesting aspects. First, the noise amplitude of the random network channel region has a smaller prefactor compared to eq 4, presumably due to −6 gate bias voltage in this case. It is a typical noise behavior of p-type CNT networks.[19] Equation 9 shows the characteristics of noise originated from the electrode−CNT contact. Note that the exponent of R_{cont} is larger than that of the randomly oriented CNT channel (eq 5). Since impurities or defect states at the electrode−CNT contact can cause excess noise,[22,23] this relatively large exponent can be presumably attributed to the imperfect contact. However, the exponent of R_{cont} is rather small just like randomly oriented CNT channel devices (eq 5) compared to that of other noise. Significantly, the noise amplitude of the aligned CNT network region $A_{R_{a\_ch}}$ follows a power law with quite a large exponent of 4.14 (eq 10), unlike the random CNT network channels which are reported to have the exponent of ∼1 (eq 8). Since there are just a few numbers of CNTs in the 100 nm width channel, this nanoscale percolative system is near percolation threshold. Previous works showed that near the percolation threshold, noise amplitude is sensitively changed according to resistance.[19,24,25] Thus, the large exponent of our empirical relation (eq 10) is consistent with several previous works.[26−29]

Using eqs 7, 8, 9, and 10, we can fit the experimental data very well, while the previously reported equation $A = 10^{-11} \times R$ cannot fit the data (Figure 4d). This indicates that the noise of CNT−electrode contacts and aligned CNT channels has quite different characteristics from that of randomly oriented CNT networks, which should be considered to properly describe the noise characteristics of arbitrary-shaped CNT network-based devices.

CONCLUSIONS

We propose a wide contact strategy to fabricate low-noise nanochannel devices based on a CNT network. We fabricated a dumbbell-shaped CNT network channel composed of a narrow long channel region and wide CNT/electrode contacts. We showed that this wide contact structure reduced the amount of noise which comes from CNT/electrode contact region. It indicates that the wide contact nanochannel devices can have the enhanced electrical properties[14] and reduced 1/*f* noise simultaneously. Interestingly, the systematic noise analysis of our devices revealed that the noise amplitude of aligned CNT network channels depends on its resistance value *R*, $\sim R^{4.14}$, which is quite different from that of random CNT networks. We provide an empirical formula that can describe the noise characteristics of arbitrary-shaped CNT network-based devices including the effect of contact resistance and CNT alignment. Our work should provide an important guideline in designing low-noise nanochannel devices for various applications such as a highly sensitive low-noise sensor.

METHODS

CNT Device Fabrication. Our CNT network-based FET arrays were fabricated following the directed assembly method as reported before (Supporting Information Figure S1).[16−18] First, photoresist (PR, AZ5214) was patterned on the SiO_2 substrate (oxide 1000 Å, Silicon Materials Inc.) *via* photolithography, and the PR-patterned substrate was dipped into octadecyltrichlorosilane (OTS, Sigma-Aldrich Inc.) solution for 10 min so that the OTS molecular layer was formed on the bare SiO_2 regions without PR. In this case, OTS solution was prepared by dissolving OTS in anhydrous hexane (Sigma-Aldrich Inc.) as 1:500 v/v concentrations. After removing the PR patterns by rinsing the substrate with acetone, the substrate was dipped into the SWNT (HiPCo, Carbon Nanotechnologies Inc.) suspensions for 10 s. In this case, the CNT suspensions were prepared by dispersing SWNTs into *o*-dichlorobenzene (Junsei Chemical Co., Ltd.) as 0.01 mg/mL concentration. Subsequently, we rinsed the substrate with *o*-dichlorobenzene and dried it by nitrogen gas. When the substrate was in the SWNT suspensions, SWNTs were selectively adsorbed onto the bare SiO_2 regions and aligned to stay inside the regions. It should be noted that, in the case of nanoscale-wide SiO_2 regions, the adsorbed SWNTs were rotated to stay in the SiO_2 regions. As a result, they were highly aligned along the channel direction. Therefore, we could fabricate the aligned CNT network channel. Last, the metal electrode (30 nm thick Au on 10 nm thick Ti) was fabricated by photolithography, thermal evaporation, and lift-off process.

Acknowledgment. This work was supported by the Korea Science and Engineering Foundation (KOSEF) grant funded by the Korea government (MEST) (No. 2010-0000799), the Conversing Research Center Program through the National Research Foundation of Korea (NRF) funded by the Ministry of Education, Science and Technology (No. 2010-K001138), System 2010 program of the MKE and Seoul R&DB program (GR070045).

Supporting Information Available: Supplementary fitting methods, additional details on fabrication method, and supplementary figures. This material is available free of charge *via* the Internet at http://pubs.acs.org.

REFERENCES AND NOTES

1. Durkop, T.; Getty, S. A.; Cobas, E.; Fuhrer, M. S. Extraordinary Mobility in Semiconducting Carbon Nanotubes. *Nano Lett.* **2004**, *4*, 35–39.
2. Javey, A.; Guo, J.; Wang, Q.; Lundstrom, M.; Dai, H. J. Ballistic Carbon Nanotube Field-Effect Transistors. *Nature* **2003**, *424*, 654–657.
3. Snow, E. S.; Novak, J. P.; Campbell, P. M.; Park, D. Random Networks of Carbon Nanotubes as an Electronic Material. *Appl. Phys. Lett.* **2003**, *82*, 2145–2147.
4. Martel, R.; Schmidt, T.; Shea, H. R.; Hertel, T.; Avouris, P. Single- and Multi-wall Carbon Nanotube Field-Effect Transistors. *Appl. Phys. Lett.* **1998**, *73*, 2447–2449.
5. Tans, S. J.; Verschueren, A. R. M.; Dekker, C. Room-Temperature Transistor Based on a Single Carbon Nanotube. *Nature* **1998**, *393*, 49–52.
6. Baughman, R. H.; Zakhidov, A. A.; de Heer, W. A. Carbon Nanotubes—The Route toward Applications. *Science* **2002**, *297*, 787–792.
7. Ghosh, S.; Sood, A. K.; Kumar, N. Carbon Nanotube Flow Sensors. *Science* **2003**, *299*, 1042–1044.
8. Guo, X. F.; Huang, L. M.; O'Brien, S.; Kim, P.; Nuckolls, C. Directing and Sensing Changes in Molecular Conformation on Individual Carbon Nanotube Field Effect Transistors. *J. Am. Chem. Soc.* **2005**, *127*, 15045–15047.
9. Hooge, F. N.; Kleinpenning, T. G. M.; Vandamme, L. K. J. Experimental Studies on 1/*f* Noise. *Rep. Prog. Phys.* **1981**, *44*, 479–532.
10. Collins, P. G.; Fuhrer, M. S.; Zettl, A. 1/*f* Noise in Carbon Nanotubes. *Appl. Phys. Lett.* **2000**, *76*, 894–896.
11. Soliveres, S.; Hoffmann, A.; Pascal, F.; Delseny, C.; Kabir, M. S.; Nur, O.; Salesse, A.; Willander, M.; Deen, J. Excess Low Frequency Noise in Single-Wall Carbon Nanotube. *Fluct. Noise Lett.* **2006**, *6*, L45–L55.
12. Behnam, A.; Bosman, G.; Ural, A. Percolation Scaling of 1/*f* Noise in Single-Walled Carbon Nanotube Films. *Phys. Rev. B* **2008**, *78*, 085431.
13. Appenzeller, J.; Lin, Y. M.; Knoch, J.; Chen, Z. H.; Avouris, P. 1/*f* Noise in Carbon Nanotube Devices—On the Impact of Contacts and Device Geometry. *IEEE Trans. Nanotechnol.* **2007**, *6*, 368–373.
14. Lee, M.; Lee, J.; Kim, T. H.; Lee, H.; Lee, B. Y.; Park, J.; Jhon, Y. M.; Seong, M. J.; Hong, S. 100 nm Scale Low-Noise Sensors Based on Aligned Carbon Nanotube Networks: Overcoming the Fundamental Limitation of Network-Based Sensors. *Nanotechnology* **2010**, *21*, 055504.
15. Lee, M.; Noah, M.; Park, J.; Seong, M. J.; Kwon, Y. K.; Hong, S. "Textured" Network Devices: Overcoming Fundamental Limitations Limitations of Nanotube/Nanowire Network-Based Devices. *Small* **2009**, *5*, 1642–1648.
16. Im, J.; Huang, L.; Kang, J.; Lee, M.; Lee, D. J.; Rao, S. G.; Lee, N. K.; Hong, S. "Sliding Kinetics" of Single-Walled Carbon Nanotubes on Self-Assembled Monolayer Patterns: Beyond Random Adsorption. *J. Chem. Phys.* **2006**, *124*, 224707.
17. Lee, M.; Im, J.; Lee, B. Y.; Myung, S.; Kang, J.; Huang, L.; Kwon, Y. K.; Hong, S. Linker-Free Directed Assembly of High-Performance Integrated Devices Based on Nanotubes and Nanowires. *Nat. Nanotechnol.* **2006**, *1*, 66–71.
18. Rao, S. G.; Huang, L.; Setyawan, W.; Hong, S. H. Large-Scale Assembly of Carbon Nanotubes. *Nature* **2003**, *425*, 36–37.
19. Snow, E. S.; Novak, J. P.; Lay, M. D.; Perkins, F. K. 1/*f* Noise in Single-Walled Carbon Nanotube Devices. *Appl. Phys. Lett.* **2004**, *85*, 4172–4174.
20. Vandamme, L. K. J.; Hooge, F. N. What Do We Certainly Know About 1/*f* Noise in MOSTs. *IEEE Trans. Electron Devices* **2008**, *55*, 3070–3085.

21. Vandamme, L. K. J.; Douib, A. Specific Contact Resistance and Noise in Contacts on Thin-Layers. *Solid-State Electron.* **1982**, *25*, 1125–1127.
22. Hooge, F. N. 1/*f* Noise Sources. *IEEE Trans. Electron Devices* **1994**, *41*, 1926–1935.
23. West, P. W. Direct-Current Method for Differentiating Contact and Bulk Low Frequency Resistance Fluctuations. *Rev. Sci. Instrum.* **1999**, *70*, 2802–2807.
24. Raychaudhuri, A. K. Measurement of 1/*f* Noise and Its Application in Materials Science. *Curr. Opin. Solid State Mater. Sci.* **2002**, *6*, 67–85.
25. Chen, C. C.; Chou, Y. C. Electrical-Conductivity Fluctuations near the Percolation-Threshold. *Phys. Rev. Lett.* **1985**, *54*, 2529–2532.
26. Garfunkel, G. A.; Weissman, M. B. Noise Scaling in Continuum Percolating Films. *Phys. Rev. Lett.* **1985**, *55*, 296–299.
27. Koch, R. H.; Laibowitz, R. B.; Alessandrini, E. I.; Viggiano, J. M. Resistivity-Noise Measurements in Thin Gold-Films near the Percolation-Threshold. *Phys. Rev. B* **1985**, *32*, 6932–6935.
28. Breeze, A. J.; Carter, S. A.; Alers, G. B.; Heaney, M. B. 1/*f* Noise through the Metal-Nonmetal Transition in Percolating Composites. *Appl. Phys. Lett.* **2000**, *76*, 592–594.
29. Kim, K.; Jang, D.; Lee, K.; Kang, H.; Yu, B. Y.; Lee, J. I.; Kim, G. T. Influence of Electrical Contacts on the 1/*f* Noise in Individual Multi-walled Carbon Nanotubes. *Nanotechnology* **2010**, *21*, 335702.
30. Myung, S.; Lee, M.; Kim, G. T.; Ha, J. S.; Hong, S. Large-Scale "Surface-Programmed Assembly" of Pristine Vanadium Oxide Nanowire-Based Devices. *Adv. Mater.* **2005**, *17*, 2361–2364.